

# THERMAL INTERRUPTION PERFORMANCE OF ULTRAHIGH-PRESSURE FREE-BURNING NITROGEN ARC

Fahim Abid<sup>1</sup>[0000-0001-8570-491X], Kaveh Niayesh<sup>1</sup>, Shashidhara Basavapura Thimmappa<sup>1</sup>,  
Camilla Espedal<sup>2</sup>, Nina Støa-Aanensen<sup>2</sup>

<sup>1</sup> Norwegian University of Science and Technology, Trondheim, Norway

<sup>2</sup> SINTEF Energy Research, Trondheim, Norway  
fahim.abid@ntnu.no

**Abstract.** In this paper, an experimental investigation of the thermal interruption performance of free-burning nitrogen arcs at 1 bar, 20 bar, and 40 bar filling pressures is reported. This work contributes to the fundamental understanding of arc characteristics at very high gas filling pressures. A resonant circuit is used to generate an arc peak current of 130 A at a frequency of 190 Hz. An ignition copper wire initiates the arc between a 4 mm diameter pin electrode and a ring electrode. The arc burns freely at a fixed inter-electrode gap of 50 mm without any forced gas flow. A resistive-capacitive branch parallel to the arc controls the initial rate of rise of recovery voltage. By changing the parallel resistance, the rate of rise of recovery voltage is varied from 9.8 V/ $\mu$ s to 84.8 V/ $\mu$ s. Time to re-ignition and the corresponding re-ignition voltages are considered as the primary parameters to characterize the thermal interruption performance. It is observed that the re-ignition time rises with the decrease of rate of rise of recovery voltage at all pressure levels, which is expected. However, in the absence of a forced gas flow, high gas filling pressure results in a reduction of the time to re-ignition and the re-ignition voltage in contrast to atmospheric pressure nitrogen arc.

**Keywords:** Supercritical fluid, Arc discharge, Free-burning arc.

## 1 Introduction

When the temperature and pressure of any fluid exceed its critical point, the fluid enters into a supercritical (SC) state [1]. Supercritical fluids exhibit properties of the gaseous phase and the liquid phase simultaneously. High density, high heat conductivity, high diffusivity, the absence of vapor bubbles and self-healing properties are some of the unique features of an SC fluid [2]. Insulation and current quenching fluids in power switching devices must hold a specific set of properties: high insulation strength during off time, low resistance during on time, large current handling capability, high voltage rating, fast recovery after switching, long lifetime, etc. For gas circuit breakers, the properties of SC fluid are believed to enhance the current interruption performance [2].

Nitrogen ( $N_2$ ) reaches a supercritical state beyond its critical pressure (33.5 bar) and critical temperature (126 K). Nitrogen is chosen in this work due to its environmentally benign nature, good insulation strength and low critical pressure. The amount of published works on arc discharge inside supercritical fluid is scarce. Nonetheless, it has been reported that the free-burning arc voltage increases with filling pressure of nitrogen, without any abrupt change during the transition from gas to SC state [3], [4]. A higher arc voltage results in a higher energy deposition in the arc channel. To the knowledge of the authors, no work has been reported on the current interruption performance of supercritical nitrogen for switchgear applications.

Current interruption can be described as a race between the cooling of the arcing channel and the voltage that builds up across the contacts. When the cooling of the arc channel is not sufficient, thermal re-ignition may occur [5]. Thermal re-ignition happens immediately after current zero (CZ) (up to a few microseconds) when the contact gap is still hot and with remaining electrical charge carriers. In contrast, dielectric re-strike happens at a much longer timescale (hundreds of microseconds) when the contact gap is fairly cold [6]. This study focuses on the influence of filling pressure on thermal re-ignition of free-burning nitrogen arcs in a fixed electrode arrangement.

Thermal re-ignition is strongly dependent on the initial rate of rise of recovery voltage (IRRRV) after CZ and the slope of the current curve before CZ [5]. In this study, the steepness of the current before CZ is kept constant. Moreover, a simplified test method is adopted by adding an impedance branch parallel to the arcing contact. A more detailed description of the method can be found in the literature [7]. By changing the resistance parallel to the arc, the IRRRV is varied from 9.8 V/ $\mu$ s to 84.8 V/ $\mu$ s. The arc is left to burn freely in  $N_2$  at 1-40 bar without any forced cooling. The thermal interruption performance will be evaluated by measuring the time to re-ignition and the voltage at re-ignition.

The test setup and the method are outlined in chapter 2. The measured time to re-ignition and re-ignition voltages as a function of IRRRV at various gas filling pressures are presented in chapter 3. Finally, in chapter 4, the conclusions are drawn from the study.

## 2 Experiment Setup

The electrical setup is shown schematically in Fig. 1. The test circuit consists of the charging and discharging sections of a 7.2  $\mu$ F high voltage (HV) capacitor bank,  $C$ . The inductance,  $L$ , and the charging voltage of  $C$  are kept constant to generate a fixed current amplitude of 130 A at a frequency of 190 Hz. Once the switch,  $S_D$ , is closed, the current flows through the inductor and further through a copper ignition wire (25  $\mu$ m diameter) inside the arcing chamber. An ignition wire is mounted between two copper tungsten (Cu-W) electrodes (pin and ring electrodes) that are kept at a fixed distance of 50 mm. Once the current flows, the ignition wire melts due to adiabatic heating and initiates the arc. The arc is allowed to burn freely between the electrodes without any forced  $N_2$  flow.

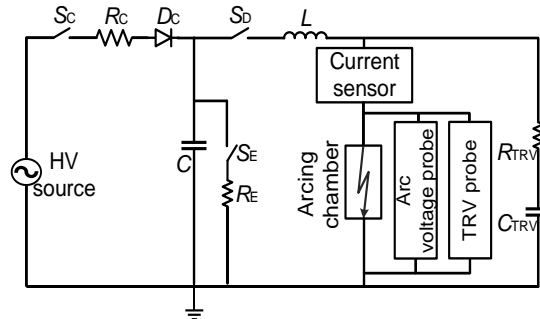


**Fig. 1.** Electrical setup consisting of a resonant circuit to generate the arc current and a TRV shaping part.

The arc current continues to flow until CZ, where the current is momentarily interrupted. Because of this momentary interruption, the energy storing elements in the circuit generate a voltage stress across the arcing contacts, known as the transient recovery voltage (TRV). In this paper, a known impedance ( $C_{TRV}$  and  $R_{TRV}$ ) parallel to the arc controls the TRV. The TRV shaping part comprises a capacitor,  $C_{TRV}$  of 1.2  $\mu\text{F}$  and a resistor,  $R_{TRV}$ . By changing  $R_{TRV}$ , the initial rate of rise of recovery voltage is controlled. Five different values of the  $R_{TRV}$  is used to generate IRRRVs in the range of 9.8  $\text{V}/\mu\text{s}$  to 84.8  $\text{V}/\mu\text{s}$ . The circuit is simulated in MATLAB Simulink to calculate the IRRRV. From the simulation, it is found that the charging voltage and the  $R_{TRV}$  are the two most important parameters influencing the IRRRV. The circuit parameters and the resulting IRRRV are shown in Table 1.

**Table 1.** Circuit parameters and the calculated current steepness and IRRRV.

L [mH]	d//dt [A/ms]	$R_{TRV}$ [ $\Omega$ ]	IRRRV [ $\text{V}/\mu\text{s}$ ]
96	152	47	9.8
		140	22.4
		280	43.0
		420	63.9
		560	84.8

Two high voltage (HV) probes with different voltage range and frequency responses are used to measure the arc voltage and TRV across the electrodes. The HV probes are connected outside the pressure tank. A shunt resistor is used to measure the arc current. The current sensor is connected on the high voltage side of the arcing chamber on a floating potential. All the data are sent to the control room via optical fiber and stored in a digital oscilloscope for further analysis. The sampling rate of the measurement is ten samples per microsecond.

Photos of the lab setup are shown in Fig. 2. The high voltage transformer, the capacitors, and the inductor can be seen in Fig. 2(a). A pressure tank of 15.7-liters rated for

500 bars, shown in Fig. 2(b), is used as arcing chamber. A 24 kV HV cable is fed through the flange of the pressure tank. The HV cable is terminated to the pin electrode and held in position inside the pressure tank by insulators. The experimental setup is put inside an explosion-safe room. The pressure tank is pressurized through the valves from the nitrogen gas bottles (black bottles in Fig. 2(b)). Before each experiment, the pressure vessel is flushed with industrial grade nitrogen, to ensure at least 99% pure nitrogen for all the experiments conducted. The ignition wire is mounted by hand for each test and is kept in the same position to reduce the experimental uncertainty. For all five circuit settings, experiments at three different pressures are conducted: 1, 20 and 40 bar. When the filling pressure is 40 bar, the fluid is in the supercritical state. Ten tests are conducted for all three pressure levels for the case where  $R_{TRV}$  is 47  $\Omega$ . For the rest of the  $R_{TRV}$  values, at least five tests are performed for each test pressure. All the operations are controlled from a separate room located at a safe distance.

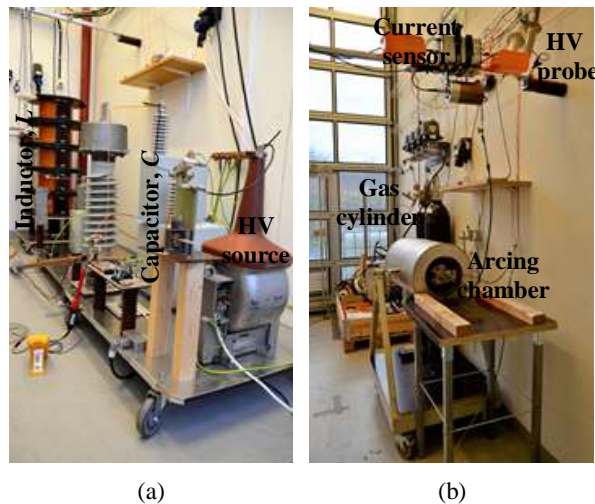


**Fig. 2.** Photos of lab setup. (a) Electrical components. (b) Arcing chamber.

### 3 Experimental Results and Discussions

A typical measurement of the arc voltage and the arc current is shown in Fig. 3. The ignition voltage peak marks the initiation of the arc. Due to the high voltage rise during ignition, some of the energy in  $C$  goes to charging  $C_{TRV}$ . Such a case of charging the TRV shaping capacitor can be seen in Fig. 3 by the collapse of the arc current during the melting of the ignition wire. However, the charging of the  $C_{TRV}$  did not have any effect on the IRRRV.

The current is interrupted momentarily at CZ (at approximately 2.6 ms). Just after CZ, the remaining charge carriers are accelerated by the rise of the TRV. Such a movement of charge carriers after CZ is often called post-arc current. If the post-arc current

is high enough, sufficient energy may remain in the hot column to re-establish the arc, seen as re-ignition in Fig. 3. The re-ignition is marked by the collapse of the TRV and by the sudden increase of the arc current. In this paper, the time between CZ and the re-ignition is defined as the time to re-ignition ( $\Delta t$ ), as shown in Fig. 3. The voltage at which the re-ignition happens is named as re-ignition voltage.

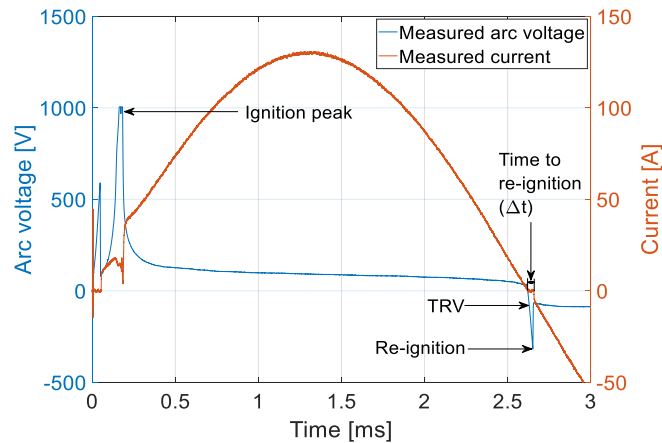


**Fig. 3.** Measured arc voltage and arc current for atmospheric pressure nitrogen arc with an arc peak current of 130 A and an IRRRV of 9.8 V/ $\mu$ s.

### 3.1 Time to Re-ignition as a Function of IRRRV

The time to re-ignition ( $\Delta t$ ) as a function of IRRRV at various filling pressures is plotted in Fig. 4. Data points at an IRRRV of 9.8 V/ $\mu$ s for all three filling pressures represent the average of ten tests while the rest of the points are the average of at least five tests. The error bar corresponds to the highest and lowest measured values of  $\Delta t$ . When the IRRRV is increased, a faster time to re-ignition is observed for all filling pressures, as expected. A higher IRRRV causes the remaining charge carriers in the arc channel after CZ to accelerate faster, which speeds up the re-ignition process. The variation in  $\Delta t$  is high when the IRRRV is low and is believed to be due to the stochastic nature of the arc discharge.

The average time to re-ignition for arcs at atmospheric pressure and an IRRRV of 9.8 V/ $\mu$ s is approximately 35  $\mu$ s. The re-ignition time goes down to approximately 13  $\mu$ s when the filling pressure is 20 bar or 40 bar. A quicker re-ignition at a high filling pressure (20 bar or 40 bar) compared to atmospheric pressure arc is also observed for all the measured IRRRV values. However, the difference in re-ignition time for arc burning in 20 bar and 40 bar gas filling pressure is less apparent.

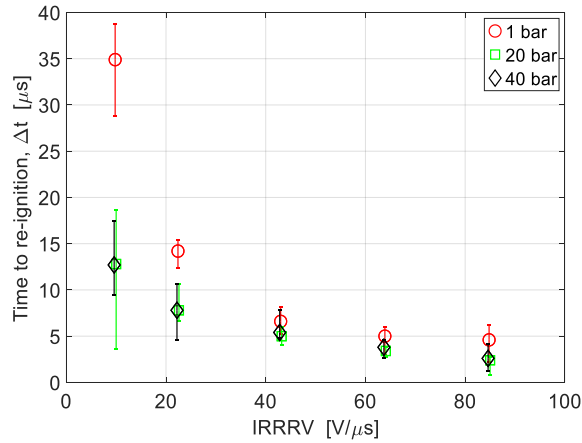


**Fig. 4.** Time to re-ignition as a function of IRRRV at different gas filling pressure.

### 3.2 Re-ignition Voltage as a Function of IRRRV

The re-ignition voltage as a function of IRRRV for different gas filling pressures is shown in Fig. 5. The average re-ignition voltage in atmospheric pressure arcs is about 250-350 V, almost irrespective of measured IRRRV ranges. The fluctuation in re-ignition voltage is less at atmospheric pressure, as indicated by fluctuation bars. The effect of high filling pressure (i.e., 20 bar or 40 bar) on the re-ignition voltage compared to atmospheric pressure is evident from Fig. 5. The average arc re-ignition voltage in 20 bar and 40 bar gas filling pressure is in the range of 50-110 V, almost irrespective of the values of the IRRRV (over the range of 9.8–84.8  $V/\mu s$ ).

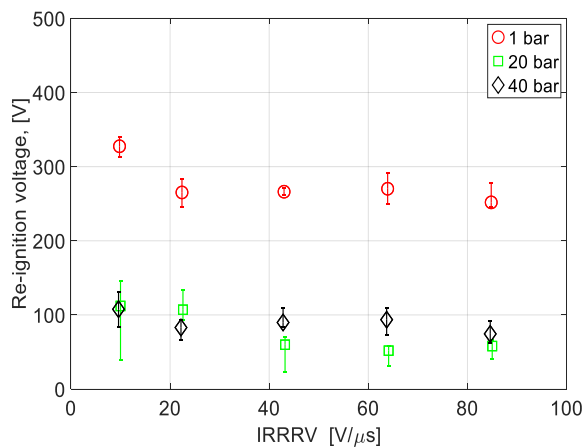


**Fig. 5.** Re-ignition voltage as a function of IRRRV at different gas filling pressures.

### 3.3 Current and Voltage Waveform Near CZ

The measured current and voltage waveforms for two different IRRRV settings at three different gas filling pressures are shown in Fig. 6. The current and arc voltage for arcs burning at different filling pressures for the IRRRV of  $9.8 \text{ V}/\mu\text{s}$  are shown in Fig. 6 (a).

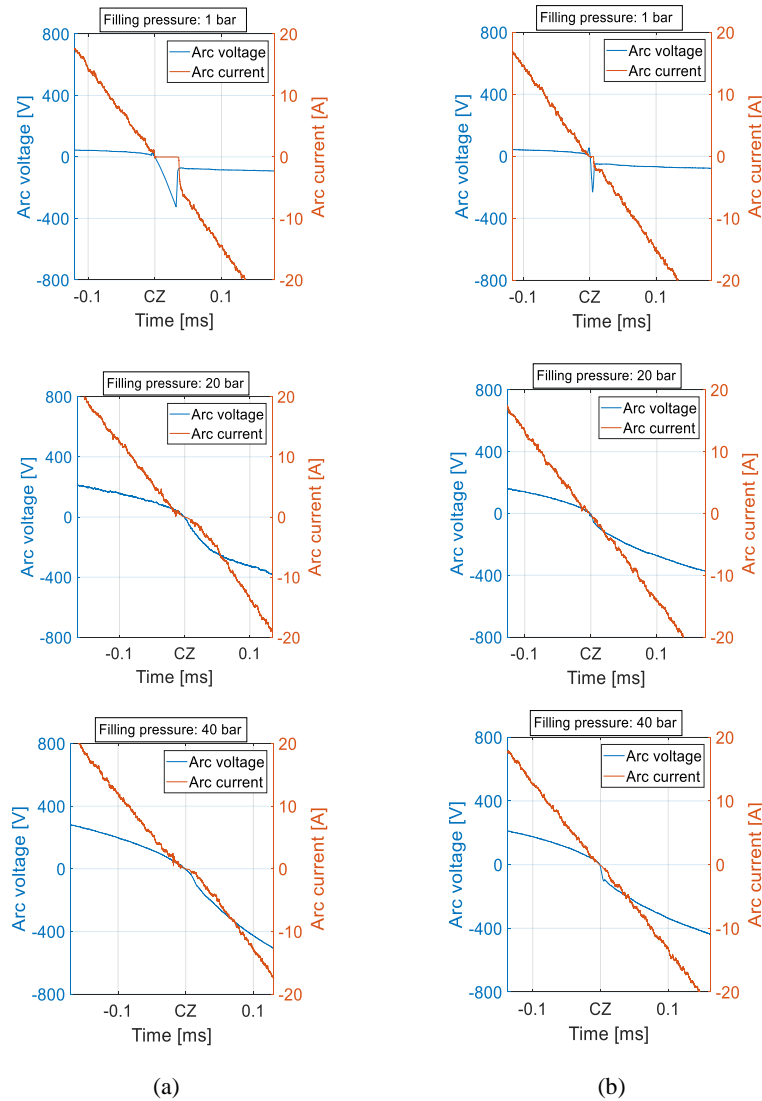


**Fig. 6.** Measured arc voltage and current waveform near CZ for different filling pressures at two different IRRRV settings. (a) IRRRV is  $9.8 \text{ V}/\mu\text{s}$ . (b) IRRRV is  $43 \text{ V}/\mu\text{s}$ .

The time to re-ignition is longer at atmospheric pressure compared to 20 and 40 bar filling pressures. At atmospheric pressure ( $\text{IRRRV} = 9.8 \text{ V}/\mu\text{s}$ ), the thermal re-ignition happens approximately  $35 \mu\text{s}$  after CZ, at a re-ignition voltage of 330 V.

For the experiments at atmospheric pressure, the re-ignition is easily detected by a distinct voltage collapse. In contrast, no sudden change in voltage can be seen at 20 and 40 bar. Here, the re-ignition is identified by a change in the slope of the measured voltage. At high pressures, the current starts to flow almost instantly after CZ. The measured arc current and the voltage waveform of the arc burning at different filling pressures for IRRRV of 43 V/ $\mu$ s is shown in Fig. 6 (b). At 1 bar, the thermal re-ignition occurs approximately 7  $\mu$ s after CZ at a re-ignition voltage of 290 V. For the arc burning at 20 bar and 40 bar; the current flows almost immediately after CZ.

The time constant of an arc is an indication of how fast the arc goes from a conducting state to an insulating state. A smaller time constant is observed as a fast change of arc voltage just before CZ. From Fig. 6, the change of arc voltage just before CZ is observed to be slower at a high gas filling pressure (i.e., 20 bar, 40 bar) compared to at 1 bar. This indicates that the time constant for free-burning arcs at higher filling pressures is larger than that at atmospheric pressure.

### 3.4 Discussions

The thermal interruption performance of free-burning nitrogen arcs is observed to worsen at high filling pressures compared to at atmospheric pressure. The current starts to flow almost immediately after CZ for arcs burning at high filling pressures (i.e., 20 bar, 40 bar). When the filling pressure increases, the arc voltages rises too. Consequently, the energy dissipation in the arc channel increases at high filling pressures. Moreover, the arc radius decreases with increasing pressure. In the absence of forced cooling near CZ, the hot core of the arc fails to dissipate the heat fast enough. The relatively high temperature of the arc core after CZ results in a high number of charge carriers which may facilitate the faster re-ignition of the arc.

The re-ignition voltage is observed to be independent of the investigated IRRRV values for a specific filling pressure. It is reported in the literature that a free-burning air arc takes almost a second to recover entirely at atmospheric pressure [8]. Under free-recovery conditions of air arcs, often the recovery voltage does not linearly increase with time. A fixed recovery voltage for some duration of time is reported in the literature [8]. In this paper, the measured re-ignition voltage of 250-350 V at atmospheric pressure is observed. The measured re-ignition voltage at atmospheric pressure is in line with the reported re-ignition voltage of nitrogen arcs of 340-350 V in the works of Nakano et al. with a different method [9].

The thermal re-ignition characteristics at 20 bar and 40 bar gas filling pressures are found quite similar. In a previous work, for arc peak current of 150 A at 350 Hz, the arc radius of the free-burning arc was calculated to be approximately 4 mm at atmospheric pressure [10]. In comparison, the calculated free-burning arc radius was 1.5 mm and 1.43 mm for arc burning at 20 bar and 40 bar respectively [10]. It was reported that the arc is constricted significantly at 20 bar filling pressure compared to at atmospheric pressure, whereas the constriction is not much when compared between the arc burning at 20 bar and 40 bar filling pressure [10]. This may explain the similarity in re-ignition properties for arcs burning at 20 bar and 40 bar filling pressure.



## 4 CONCLUSIONS

The thermal interruption performance of free-burning nitrogen arcs as a function of  $N_2$  filling pressure is reported in this paper. By adding a resistive-capacitive branch parallel to the arc, the IRRRV is controlled, whereas the slope of the current decay before CZ is fixed. The time to re-ignition and the re-ignition voltages are analyzed as a function of IRRRV at different filling pressures. Based on the experimental investigations, the following conclusions have been drawn:

- The time to re-ignition increases when the IRRRV decreases for all gas filling pressures, as expected.
- High nitrogen filling pressures (i.e., 20 bar, 40 bar) reduce the time to re-ignition compared to atmospheric pressure arc.
- The re-ignition voltage is not strongly dependent on the investigated IRRRV values. The re-ignition voltage is found to decrease at high filling pressures (i.e., 20 bar, 40 bar) compared to free-burning arcs in atmospheric pressure.
- The thermal interruption performance of free-burning arcs worsen at high nitrogen filling pressures compared to atmospheric pressure arc.

## Acknowledgement

This work is supported by the Norwegian Research Council.

## References

1. D. Banuti, M. Raju, P. C. Ma, M. Ihme, and J.-P. Hickey, "Seven questions about supercritical fluids - towards a new fluid state diagram," presented at the 55th AIAA Aerospace Sciences Meeting, 2017.
2. J. Zhang, A. Markosyan, M. Seeger, E. van Veldhuizen, E. van Heesch, and U. Ebert, "Numerical and experimental investigation of dielectric recovery in supercritical  $N_2$ ," *Plasma Sources Science and Technology*, vol. 24, no. 2, p. 025008, 2015.
3. F. Abid, K. Niayesh, E. Jonsson, N. S. Støa-Aanensen, and M. Runde, "Arc Voltage Characteristics in Ultrahigh-Pressure Nitrogen Including Supercritical Region," *IEEE Transactions on Plasma Science*, vol. 46, no. 1, pp. 187-193, 2018.
4. F. Abid, K. Niayesh, E. Jonsson, N. S. Støa-Aanensen, and M. Runde, "Arc Voltage Measurements Of Ultrahigh Pressure Nitrogen Arcs In Cylindrical Tubes," presented at the 22nd International Conference on Gas Discharges and their Applications, Novi Sad, Serbia, 2-7 September 2018.
5. K. Niayesh and M. Runde, *Power Switching Components*. Springer, 2017.
6. H. Edels, A. Halder, A. Shaw, and D. J. N. Whittaker, "Convection-free post-arc gap recovery," vol. 193, no. 4812, p. 263, 1962.
7. A. Karimi and K. Niayesh, "A simple evaluation method of the thermal interruption limit of power circuit breakers," *Electrical Engineering*, vol. 90, no. 8, pp. 523-528, 2009.
8. F. Crawford and H. Edels, "The reignition voltage characteristics of freely recovering arcs," *Proceedings of the IEE-Part A: Power Engineering*, vol. 107, no. 32, pp. 202-212, 1960.

9. T. Nakano, Y. Tanaka, K. Murai, Y. Uesugi, T. Ishijima, K. Tomita, K. Suzuki and T. Shinkai, "Thermal re-ignition processes of switching arcs with various gas-blast using voltage application highly controlled by powersemiconductors," *Journal of Physics D: Applied Physics*, vol. 51, no. 21, p. 215202, 2018.
10. F. Abid, K. Niayesh, and N. Støa-Aanensen, "Ultrahigh-Pressure Nitrogen Arcs Burning inside Cylindrical Tubes," *IEEE Transactions on Plasma Science*, vol. 47, no. 1, pp. 754-761, Jan. 2019.